Research on Engineering Structures & Materials
www.jresm.org
Research Group

Research Article

Evaluation of damping reduction factors for displacement and acceleration spectra using code-compatible near-fault and far-fault ground motions depending on site conditions

Abdelmalek Abdelhamid[1,2,a], Baizid Benahmed[*1,b], Omar Laghrouche[3,c], Mehmet Palanci[4,d], Lakhdar Aidaoui[1,e]

[1]*Development Laboratory in Mechanics and Materials, University of Djelfa, Djelfa, Algeria*
[2]*Department of Science & Technology, University of Tissemsilt, Tissemsilt, Algeria*
[3]*Institute for Infrastructure and Environment, Heriot-Watt University, Edinburgh, UK*
[4]*Civil Engineering Department, Istanbul Arel University, Istanbul, Turkey*

Article Info

Article history:

Received 09 Feb 2024
Accepted 15 June 2024

Keywords:

Damping reduction factors;
Ground motion selection;
Response spectra;
Site conditions;
EC8

Abstract

Damping Reduction Factors (DRFs) are widely employed in design standards to adjust the structural response due to varied levels of the structural damping, higher or lower than the common value of 5% for response spectra or time history analyses. Research findings highlighted that DRFs are sensitive not only to damping and period, but also to the seismological parameters and site conditions. Nevertheless, effect of ground motions on the DRFs compiled to code-based target spectrum are not investigated. For this purpose, Eurocode-8 (EC8) compatible real ground motions were carefully selected for three soil classes, namely, A, B, and C, considering near- and far-fault ground motions and DRFs were derived from the displacement and acceleration response spectra through, Single Degree of Freedom (SDOF) systems, dynamic analyses. Near- and far-fault ground motions were considered to investigate the effect of the distance on DRFs. The distributions of DRFs were then subjected to a comparison with code-based and existing literature DRF models and bias between the models were calculated. The findings demonstrated that near- and far-fault ground motions produced different outcomes and DRFs obtained from acceleration spectra were, on average, approximately 25% higher than those obtained from displacement spectra. It was also observed that DRFs were sensitive to soil classes, especially to soil class B. The maximum near/far fault ratios determined for site class B were 1.20, 1.45 and 1.71 for damping ratios of 10, 20, and 40%, respectively. In addition, results indicated that the DRF values provided by EC8 were generally non-conservative. Therefore, it is important that the code-based definitions should be refined to consider important parameters that affect DRFs such as distance and soil classes.

1. Introduction

Response spectrum analysis is one of the most widespread seismic design approaches in earthquake engineering, using a viscous damping ratio of 5%. To perform such analysis to other damping ratios, DRFs are used, and seismic codes define DRFs as function of damping ratio and structural period. On the other hand, recent studies have shown that the DRFs are also sensitive to seismological characteristics such as magnitude, distance, near- and far-fault ground motion, fault type, near-source forward directivity, and site conditions etc. [1]–[3]. Therefore, empirical expressions are proposed. However, most of these parameters have not been taken into consideration in seismic codes yet.

*Corresponding author: benahmed.tp@univ-djelfa.dz
[a] orcid.org/0009-0004-2414-070X; [b] orcid.org/0000-0003-4924-0059; [c] orcid.org/0000-0002-2439-2753; [d] orcid.org/0000-0002-9223-5629; [e] orcid.org/0000-0003-0488-3800
DOI: http://dx.doi.org/10.17515/resm2024.153ea0209rs

Firstly, Newmark and Hall [4], [5] proposed the first formulation for the DRFs that has been adopted in many standards and codes, for example, ATC-40 [6], FEMA-273 [7], UBC (1997) [8], ASCE7-05 (2006) [9], and FEMA-356 [10]. Kawashima and Aizawa [11] findings were introduced in the Caltrans Seismic Design Criteria [12]. Ashour's [13] relationship has been introduced in UBC (1994) [14] and NEHRP [15]. Bommer *et al.* [16] formulation was adopted in EC8 [17]. The equation of Ramirez *et al.* [18] was implemented in NEHRP [19] and that of Otani and Kanai [20] has been adopted in the Japanese Seismic Design Code [21]. Priestley [22] suggested an empirical formula that takes into consideration the structural period and near-fault (NF) ground motion for a modified version of EC8. The Zhou *et al.* [23] model was acknowledged in Chinese seismic code [24]. Benahmed [25] proposed an expression of the DRF based on a nonlinear regression, which was introduced in the Algerian Seismic Regulation (RPA 99 version 2003) [26] considering the structural period and damping ratio.

Besides the studies on improving DRF values, Hubbard and Mavroeidis [27] concluded that the DRF models proposed in most standards and codes are based on far-fault (FF) seismic excitation, and these DRF values are non-conservative for NF records. They formulated a conservative model by utilizing NF motions characterized by diverse velocity pulses. Pu *et al.* [28] stated that DRFs derived from FF motions are not appropriate to be used in a design for NF effects and this situation can lead to erroneous results. Li and Chen [29] stated that DRF values derived from FF motion in NF cases may lead to accuracy problems. In addition, Atkinson and Pierre [1] have found that DRFs are sensitive to the moment of magnitude and distance. Based on Hatzigeorgiou [2], on the other hand, DRFs were independent of the distance, but sensitive to soil types ranging from hard rock to soft soil.

Lin and Chang [30] investigated the soil conditions, according to the NEHRP soil classification, and their impact on DRFs obtained from displacement (DRFd) and acceleration (DRFa) response spectra. They concluded that the DRFs derived from displacement spectra were very similar for A, B, and D soil classes, whereas for C soil class, they were slightly different. In addition, it was indicated that DRFa values are more vulnerable to soil conditions than DRFd values. They suggested that DRFa should be used when the structural damping ratio determined from the hysteretic behavior. Otherwise, DRFd must be used if high levels of damping are implemented into the structure when using energy dissipation devices. Hatzigeorgiou [2] stated that the existing methods proposed for DRFs from displacement (Sd) and pseudo-acceleration (PSa) spectra provide a good correlation with the displacement response. This is crucial for high-damping systems because smaller DRFs are obtained from PSa spectra and may cause a significant underestimation of the seismic design forces. Accordingly, the different DRFs should be adopted.

Hao *et al.* [3] concluded that moment magnitude has a notable impact on the DRFs compared to the closest distance and site conditions, especially for classes B-D according to NEHRP [19]. Moreover, these parameters had more influence on DRFa compared to DRFd and DRFv. Zhao *et al.* [31] noticed that the impact of earthquake characteristics and soil types on DRFa are similar to those DRFd for a spectral periods up to 0.3s. At spectral periods longer than 0.3s, earthquake characteristics and soil conditions have a larger impact on DRFa compared to DRFd. Davila and Mendo [32] determined that significant differences exist in the DRFs computed from displacements compared to those computed from acceleration and velocity for periods greater than 0.2s. They found that the values of DRFd for site classes S1, S2, and S3 as per the ASCE 7-16 [33] exhibit similarity and can be adequately approximated by their average for all damping ratios and periods higher than 2.0s. They highlighted that this was not valid for DRFa and DRFv specifically for damping ratios higher than 20%. It was suggested that deriving DRF equations from acceleration and velocity response spectra specific to each soil tyoe would be more appropriate.

Benahmed [34] investigated the damping uncertainty effects on the DRFs for both displacement and acceleration response spectra. It was highlighted that the DRFd values are more susceptible to the uncertainties inherent in damping than the DRFa values. Also, Abdelhamid *et al.* [35] have studied the uncertainties in DRFs using artificial neural networks for acceleration, velocity, and displacement spectra. Their conclusion highlighted that DRFs derived from acceleration spectra exhibit greater sensitivity to the inherent damping uncertainties compared to DRFs derived from displacement and velocity spectra.

Benahmed [25] found that there is a weak dependency between the DRFs from different soil types and concluded that the influence of the soil type can be omitted. Pavlou and Constantinou [36] examined the accuracy of DRFs implemented in NEHRP when applied to NF motions; however, they did not propose any equations. Daneshvar and Bouaanani [37] considered eastern Canada ground motions for the proposition of a DRFs empirical expression for a wide range of damping ratios, from 1% to 40%, taking into account magnitude, distance, and soil types. The obtained DRFs were dependent on the spectral period and magnitude at high periods, while the effect of distance was observed to have a limited impact. Different studies can be also found in the literature that investigate and propose DRF equations considering different structures, soil types, seismological effects etc. [38]–[43].

UBC97 [8] is the first seismic code to specify consideration of NF effects. It defines near-source factors based on source type and closest distance to the known seismic source. In the Chinese seismic code [24], construction sites are categorized into three groups based on the proximity to the ruptured fault and it recommends to use a larger response spectrum for closer ruptured faults. It is clear that increasing the response spectrum amplification leads to a more conservative design.

1.1 Contribution of the Paper

Discussions of the above studies indicate that the dependency of the DRFs on the different considered parameters does lead to different conclusions. Therefore, based on the ground motion database and building topologies, the influence of different seismological and geotechnical factors on DRFs needs further investigation. In addition, the relationship between NF and FF motions and their impact on dynamic response factors remain as open questions. For example, are DRF values observed for NF and FF motions comparable, or is there a significant difference? Do DRFs vary between the values derived from acceleration spectra and those derived from displacement spectra? Can we overlook the impact of soil type on DRFs? In addition to these open questions, the effect of NF and FF ground motions on DRFs are not evaluated in terms of code-compatible ground motions. Accordingly, this is the first study that investigates the effects of NF and FF motions on DRFs considering the spectral shape defined in the seismic code.

For this purpose, the present study investigates the influence of the NF and FF motions on DRFs considering different soil classes of EC8 design spectra. Real earthquake ground motions were taken from European Strong Motion Database [44] and Pacific Earthquake Engineering Research (PEER) Database [45]. These were grouped into six categories considering NF and FF motions as well as site classes of A, B, and C defined in EC8. Selected records were then subjected to a spectral matching algorithm developed by Kayhan et al. [46] and code-compatible ground motions records were obtained. Linear dynamic analyses were conducted for damping ratios of 5%, 10%, 20%, and 40% to determine DRFs using displacement and acceleration response spectra. The obtained results were then analysed and compared with DRF equations recommended in EC8 and two other known prediction equation models found in the literature [2], [30].

2. Selection of Ground Motions

Ground motion selection is an integral method for the success of time history analysis [47]–[51]. Appropriately selected records, for a given soil class considering seismological parameters, increase the accuracy and lead to realistic results [46]. According to Graizer and Kalkan [52], several earthquake characteristics that have an effect on the accelerogram spectral shape should be considered. Since there is no specific building or building group used in this study, the period interval for spectral matching was assumed between 0.1s and 4.0s which covers different heights of buildings. Three soil classes, namely, A, B, and C defined in EC8 were considered and earthquake records were classified according to shear wave velocity $V_{s,30}$ as given in Table 1. By this way, the influence of site conditions on DRFs will be examined. NF records were acquired when ground motions were within 20 km of the epicenter, while FF records were gathered for ground motions at epicentral distance exceeding 20 km. Pulse-like motion effects were not taken into account in this study. Using the different ground motion source databases [44], [45], ground motion records were collected (see Fig. 1). Based on the sources, moment magnitude of the records in the database varied between 5.2 and 7.7. Ground motion records were then post processed by the software developed by Kayhan *et al.* [46] to obtain code-compatible records for the analyses.

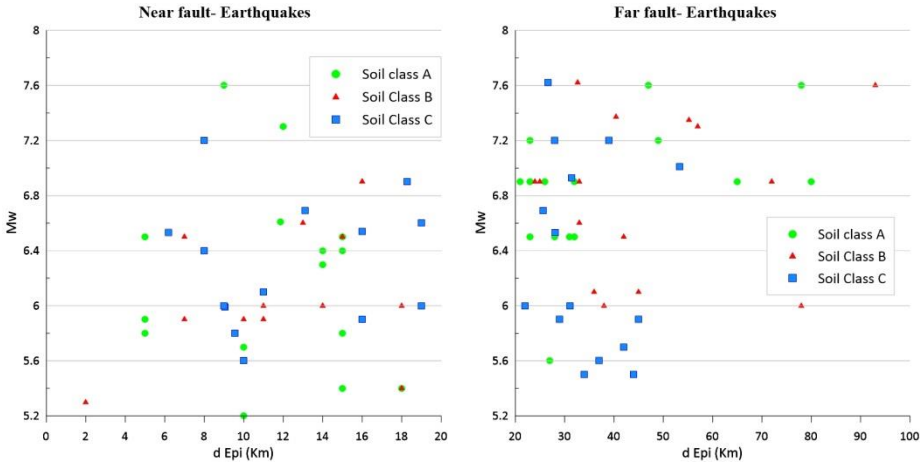

Fig. 1. The distribution of moment magnitude against epicentral distance for selected earthquakes, (left) near-fault and (right) far-fault

DRFs were computed from the acceleration and displacement response spectra of SDOF systems for each of the horizontal components of the records separately (i.e., unidirectional analysis was performed) for both NF and FF records (see Tables 2 to 4). It was difficult to choose original ground motions owing to strict constraints such as moment magnitude, soil categorization, and target spectrum. As a result, original ground motion records were, when necessary, scaled. Records selection constraints and procedures defined in the code [17] were used as input in the software and a total of 15 scaled records for each soil group were determined that match the target design spectrum. The target spectrum was constructed using 5% damping ratio and a peak ground acceleration of 0.35g. Although the effect of scaling factors were found statistically independent of the building responses, if the spectral shape matching is satisfied [53], [54], [55], it is worth stating that the scaling factors (used when necessary) were less than 2.0 [47], [48], [56]. It should be noted that an in-house computer program coded by the authors were used for the linear analysis of earthquakes using the Newmark's step by step time integration method [57]. Spectral acceleration and displacement history of selected earthquakes (i.e.,

S_a and S_d) for the period interval between 0.02s and 4.00s with increments of 0.02s considering the damping ratios of 5%, 10%, 20% and 40%, were computed by this program.

Table 1. Soil classes defined in EC8 [17]

Soil Class	Description of ground type	Vs,30 (m/s)	NSPT (bl/30cm)	Cu (kPa)
A	Rock or other rock-like geological formation, including at most 5 m of weaker material at the surface.	> 800	-	-
B	Deposits of very dense sand, gravel, or very stiff clay, at least several tens of meters in thickness, characterized by a gradual increase of mechanical properties with depth.	360 - 800	> 50	> 250
C	Deep deposits of dense or medium dense sand, gravel or stiff clay with thickness from several tens to many hundreds of meters.	180 - 360	15 - 50	70 - 250

The list of selected records, for each soil type for both cases of NF and FF earthquake records, are listed in Tables 2 to 4. The acceleration spectrum of EC8, the spectral acceleration of obtained ground motions and their mean corresponding to site classes are plotted in the Figures 2 to 4.

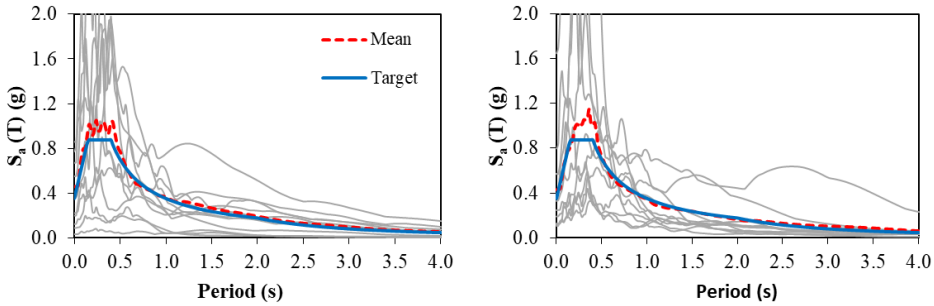

Fig. 2. Response spectral acceleration of ground motions matching with EC8 target spectrum considering NF (left) and FF (right) records for site class A

Table 2. Characteristics of earthquakes obtained for NF and FF records for soil class A

Near Fault					Far Fault				
Comp	Earthquake	M_w	Station	d_{Epi} (km)	Comp	Earthquake	M_w	Station	d_{Epi} (km)
X	South Iceland (aftershock) 21/06/00	6.4	ST2557	15	Y	South Iceland 17/06/00	6.5	ST2496	31
Y	South Iceland (aftershock) 21/06/00	6.4	ST2496	14	Y	Izmit 17/08/99	7.6	ST770	78
Y	Izmit 17/08/99	7.6	ST575	9	Y	Montenegro 15/04/79	6.9	ST64	21
Y	Valnerina 19/09/79	5.8	ST225	5	X	South Iceland 17/06/00	6.5	ST2557	32

X	Bingol 01/05/03	6.3	ST539	14	X	Campano Lucano 23/11/80	6.9	ST102	80
Y	Mt. Hengill Area 04/06/98	5.4	ST2495	18	Y	Campano Lucano 23/11/80	6.9	ST96	32
Y	Mt. Hengill Area 04/06/98	5.4	ST2497	15	Y	Umbria 29/04/84	5.6	ST138	27
Y	South Iceland 17/06/00	6.5	ST2558	15	Y	Vrancea 30/08/86	7.2	ST40	49
Y	Tabas 16/09/78	7.3	ST54	12	X	Avej 22/6/2002	6.5	ST3311	28
Y	NE of Banja Luka 13/08/81	5.7	ST2950	10	Y	Duzce 1 12/11/99	7.2	ST3136	23
X	South Iceland 17/06/00	6.5	ST2486	5	X	Friuli 06/05/76	6.5	ST20	23
X	Lazio Abruzzo 07/05/84	5.9	ST140	5	X	Campano Lucano 23/11/80	6.9	ST100	26
Y	Calabria 11/03/78	5.2	ST45	10	Y	Montenegro 15/04/79	6.9	ST68	65
PUL164	San Fernando1 09/02/71	6.61	Pacoima Dam	11.86	X	Izmit 17/08/99	7.6	ST561	47
Y	Izmit (aftershock) 13/09/99	5.8	ST575	15	Y	Campano Lucano 23/11/80	6.9	ST93	23

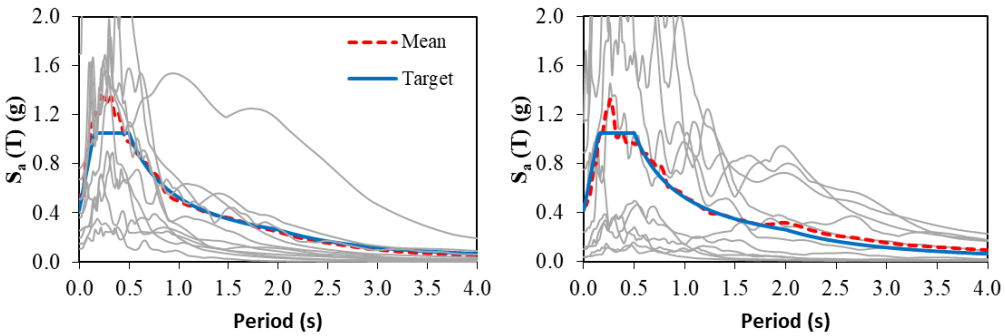

Fig. 3. Response spectral acceleration of ground motions matching with EC8 target spectrum considering NF (left) and FF (right) records for site class B

Table 3. Characteristics of earthquakes obtained for NF and FF records for soil class B

Near Fault					Far Fault				
Comp	Earthquake	M_w	Station	d_{Epi} (km)	Comp	Earthquake	Mw	Station	d_{Epi} (km)
Y	South Iceland 17/06/00	6.5	ST2482	15	X	Campano Lucano 23/11/80	6.9	ST99	33
Y	Firuzabad 20/06/94	5.9	ST3297	7	X	Aigion 15/06/95	6.5	ST1332	42
X	Skydra-Edessa 18/02/86	5.3	ST1306	2	X	Montenegro 15/04/79	6.9	ST63	24
Y	Ano Liosia 07/09/99	6	ST1258	14	X	Montenegro 15/04/79	6.9	ST62	25

Y	Kalamata 03/01/04	5.9	ST164	10	X	South Aegean 23/05/94	6.1	ST1310	45
X	Ano Liosia 07/09/99	6	ST1257	18	X	Umbria Marche 26/09/97	6	ST231	78
X	Ano Liosia 07/09/99	6	ST1259	14	Y	Panisler 30/10/83	6.6	ST133	33
Y	Campano Lucano 23/11/80	6.9	ST276	16	CHY028 -E	Chi-Chi, Taiwan 21/09/99	7.62	CHY028	32.67
X	Montenegro 15/04/79	5.4	ST63	18	1875y	Griva 21/12/90	6.1	ST1306	36
Y	Kalamata 03/01/04	5.9	ST163	11	ABBAR-T	Manjil, Iran 21/06/90	7.37	ABBAR	40.43
X	Erzincan 13/03/92	6.6	ST205	13	TAB-LN	Tabas, Iran 16/09/78	7.35	Tabas	55.24
Y	Patras 14/07/93	5.6	ST1330	10	Y	Campano Lucano 23/11/80	6.9	ST103	72
Y	South Iceland 17/06/00	6.5	ST2484	7	X	Tabas 16/09/78	7.3	ST59	57
Y	Montenegro 15/04/79	6.9	ST67	16	Y	Izmit 17/08/99	7.6	ST544	93
Y	Umbria Marche 26/09/97	6	ST60	11	Y	Umbria Marche 26/09/97	6	ST228	38

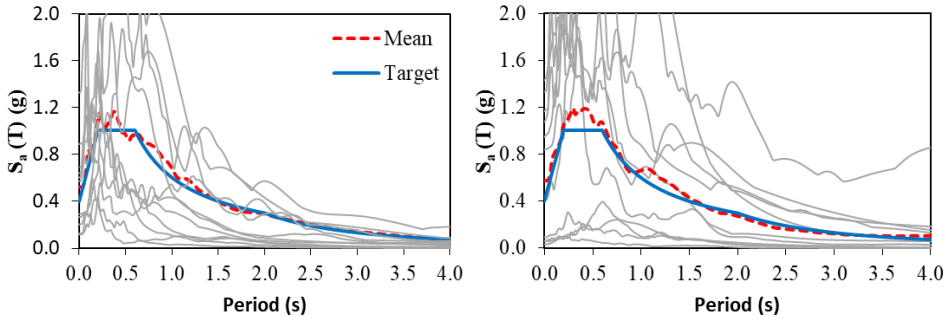

Fig. 4. Response spectral acceleration of ground motions matching to EC8 target spectrum considering NF (left) and FF (right) records for site class C

Table 4. Characteristics of earthquakes obtained for NF and FF records for soil class C

Near Fault					Far Fault				
Comp	Earthquake	M_w	Station	d_{Epi} (km)	Comp	Earthquake	M_w	Station	d_{Epi} (km)
X	Faial 07/09/98	6.1	ST87	11	Y	Cubuklu 17/08/99	5.5	ST65	34
Y	Lazio Abruzzo 07/05/84	5.9	ST147	16	H-E08140	Imperial Valley 15/10/79	6.53	Imperial Valley-06	28.09
A-OBR270	WHITTIER NARROWS 01/10/87	5.99	OBREGON PARK	9.05	PAR—L	Northridge 01 17/01/94	6.69	Pardee – SCE	25.65
X	Friuli 06/05/76	6	ST33	9	Y	Lazio Abruzzo 07/05/84	5.9	ST148	45

X	Ano Liosia 07/09/99	6	ST1253	19	RIO360	Cape Mendocino 25/04/92	7.01	RIO DELL OVERPAS	53.34
Y	Dinar 01/10/95	6.4	ST271	8	X	Duzce 1 12/11/99	7.2	ST3139	28
X	Alkion 2/25/81	6.6	ST122	19	Y	Seferihisar 10/04/03	5.7	ST858	42
KJM000	Kobe, Japan 17/01/95	6.9	KJMA	18.27	X	Duzce 1 12/11/99	7.2	ST541	39
Y	Duzce 1 12/11/99	7.2	ST553	8	TCU065 -E	Chi-Chi, Taiwan 21/09/99	7.62	TCU065	26.67
X	Patras 14/07/93	5.6	ST10	10	C02065	PARKFIELD1 28/09/04	6	CHOLAM E	31.04
H-BCR230	Imperial Valley 15/10/79	6.53	BONDS CORNER	6.2	Y	Patras 14/07/93	5.6	ST215	37
NGI270	San Salvador 13/02/01	5.8	NATL GEOGRAF ICAL INST	9.54	G03000	Loma Prieta 18/10/89	6.93	GILROY ARRAY	31.4
SCS052	Northridge 17/01/94	6.69	SYLMAR-CONVERT ER	13.11	Y	Chenoua 29/10/89	5.9	ST2881	29
B-PTS225	Superstition Hills 24/11/87	6.54	Parachute Test Site	15.99	X	Umbria Marche 26/09/97	6	ST223	22
X	Umbria Marche 26/09/97	5.5	ST221	7	X	Filippias 16/06/90	5.5	ST126	44

3. Results and discussions

3.1 DRF Models Used for Comparison Analysis

In this section, Lin and Chang [30] (called LC04 hereafter) and Hatzigeorgiou [2] (called H10 hereafter) models are presented and compared with the results obtained in this study since these models consider the influence of soil conditions.

As already mentioned, DRFs are adjusting factors to be applied to the 5% damped spectral ordinates and they are frequently obtained from the different viscous damping considering the displacement response of elastic SDOF systems as given in (Eq. 1). In addition to (Eq. 1), DRFs can also be calculated by two other definitions (Eq. 2), namely, pseudo-spectra related to displacement of the structure, which are the pseudo-velocity spectrum S_{pv} and pseudo-acceleration spectrum S_{pa}. They are often used to study the true response spectra (S_v and S_a) to construct the design spectra [28].

$$S_{pv}(T,\xi) = \frac{2\pi}{T} S_d(T,\xi) \tag{1}$$

$$S_{pa}(T,\xi) = \frac{2\pi}{T} S_v(T,\xi) = \frac{4\pi^2}{T^2} S_d(T,\xi) \tag{2}$$

DRFs adopted by seismic codes are often defined as the ratio between the displacement or acceleration spectra, $S_d(T,\xi)$ or $S_a(T,\xi)$, and 5% damped displacement or acceleration spectrum, $S_d(T,5\%)$ or $S_a(T,5\%)$, respectively, as described in (Eq. 3) and (Eq. 4) [2], [3], [29], [30].

$$DRFd(T,\xi) = \frac{S_d(T,\xi)}{S_d(T,5\%)} = \frac{S_{pa}(T,\xi)}{S_{pa}(T,5\%)} \tag{3}$$

$$DRFa(T,\xi) = \frac{S_a(T,\xi)}{S_a(T,5\%)} \tag{4}$$

In EC8, the damping effect is introduced via the damping correction factor (η) defined by (Eq. 5) and η=1 for the reference value of 5% viscous damping. In the equation, the damping ratio is expressed in percentage and the damping correction factor should be equal or greater than 0.55, as recommended by EC8.

$$\eta = \sqrt{10/(5+\xi)} \tag{5}$$

Lin and Chang [30] have performed a statistical study to predict the damping reduction factors considering 1037 seismic records on three types of soil classes (A to D) according to NEHRP [15]. The proposed models are given in (Eq. 6) and (Eq. 7). They are based on the spectrum different constant values which are used to estimate the DRFs (see Tables 5 and 6).

$$DRFd = 1 - \frac{aT^b}{(T+1)^c} \tag{6}$$

Table 5. Site- and damping-dependent coefficients for DRFd [30]

Site class	*a*	*b*	*c*
AB	1.1637+0.3885ln(ξ)	0,229	0.505
C	1.4532+0.4872ln(ξ)	0.354	0.810
D	1.3243+0.4426ln(ξ)	0.311	0.664

Hatzigeorgiou [2] proposed a new model (Eq. 8) to predict DRFs dependent on displacement and acceleration response spectra accounting the impact of soil and ground motion types (i.e., NF and FF earthquakes), in addition to viscous damping ratio and vibration period. c_1 to c_5 are the constants of equation and they are given in the Tables 7 and 8 for DRFd and DRFa, respectively.

$$DRFa = d + eT \tag{7}$$

Table 6. Site- and damping-dependent coefficients for DRFa [30]

Site class	*d*	*e*
AB	$0.391\xi^{-0.304}$	$0.0057+0.383\xi-1/15{,}929\xi^2$
C	$0.309\xi^{-0.392}$	$0.0151+0.474\xi-1/10{,}241\xi^2$
D	$0.326\xi^{-0.371}$	$0.0348+0.248\xi-1/8{,}250\xi^2$

$$DRF(T,\xi) = 1 + (\xi - 5)\cdot[1 + c_1\cdot ln(\xi) + c_2\cdot(ln(\xi))^2] \cdot [c_3 + c_4\cdot ln(T) + c_5\cdot(ln(T))^2] \tag{8}$$

Table 7. Coefficient values in (Eq. 8) for DRFs dependent on displacement spectra [2]

	Far-fault			Near-fault
	Site A	Site B	Site C	All Site classes
c_1	-0.30453	-0.29404	-0.29406	-0.30241
c_2	0.2184	0.01963	0.0199	0.02183
c_3	-0.07729	-0.09299	-0.09014	-0.08926
c_4	0.00229	0.00897	-0.00001	0.01097
c_5	0.00229	0.01219	0.01196	0.01007

Table 8. Coefficient values in (Eq. 8) for DRFs dependent on acceleration spectra [2]

	Far-fault			Near-fault
	Site A	Site B	Site C	All Site classes
c_1	-0.36725	-0.36051	-0.36128	-0.36227
c_2	0.03526	0.03498	0.03494	0.03495
c_3	-0.02634	-0.04093	-0.05435	-0.04517
c_4	0.0323	0.03379	0.02907	0.03454
c_5	-0.01047	-0.00191	0.00612	-0.0024

3.2 Effect of Near- And Far-Fault Ground Motions on the DRFd

In Figures 5 to 7, the mean values of the DRFs calculated for NF and FF earthquakes and all ground motions (i.e., combination of results of near- and far-faults) for a structural damping ratio of 10%, 20%, and 40%, are plotted separately. It can be stated from the figures that DRFd values generally increase with increasing damping ratios and vibration periods.

Figure 5 shows the trend of the computed DRFs as well as the predictive models and it is seen that the LC04 model is comparable with NF and FF DRFs. The trend of the H10 model seems to be in agreement with DRFs for NF earthquakes, but DRFs produced by the H10 model for FF earthquakes is not satisfactory compared to the NF results. The misfit of FF DRFs increases with increasing damping ratio. Since the EC8 model is not dependent on the periods, the values are constant for all periods and DRFs are decreasing with increasing damping. According to Figure 5, target DRFs fluctuated around DRFs produced by EC8 for damping ratio lower than 40%, implying less misfit between them.

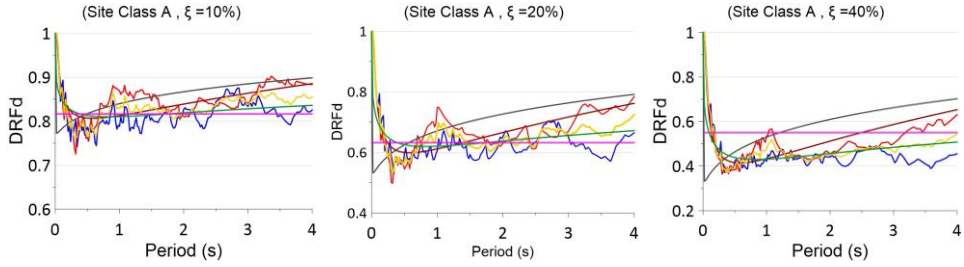

Fig. 5. DRFd values for NF and FF earthquakes for soil A

DRFd values obtained for soil B are plotted in Figure 6 with code-based results and prediction models. It is observed that the H10 model slightly differs from the analysis results for soil B for T > 2.0s and damping ratios of 10% and 20%. Distribution of DRFd values between NF and FF motions diverged and this becomes more evident with increasing damping ratios in soil B Compared to soil A. DRFd values of NF motions are greater than those of FF motions by 16%, 38%, and 58%, for ξ=10%, 20% and 40%, respectively. Compared to soil B, DRFd values, calculated for NF and FF earthquakes shown in Figure 7, are less scattered in soil C. It appears that the accuracy of LC04 and H10 models increases and the H10 model seems slightly in better agreement with target DRFs compared to LC04 and this becomes more evident for high natural periods and damping ratios. It is obvious from the figures that DRFd values according to the EC8 definition are non-conservative, especially for T > 1.5s and ξ ≤ 20%. Owing to the fixed condition given by EC8 ($\eta \geq 0.55$), the DRFd values provided by the code are conservative since the code-based values are larger than the target values for 40% damping, especially for periods less than 3s for A and B soil types, and periods less than 2.5s for C soil type.

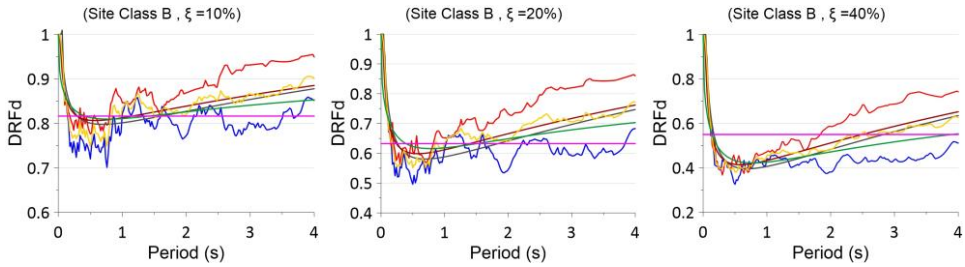

Fig. 6. DRFd values for NF and FF earthquakes for soil B

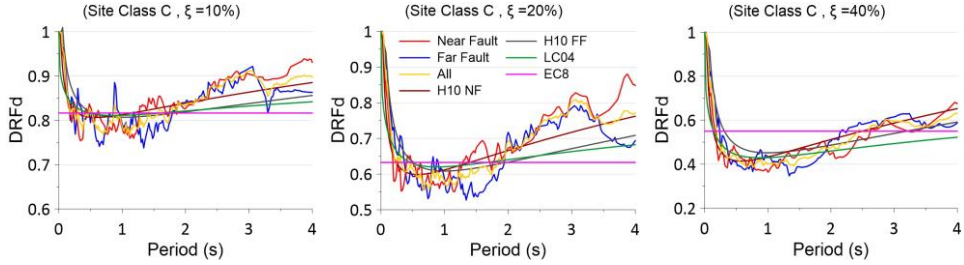

Fig. 7. DRFd values for NF and FF earthquakes for soil C

To examine the results quality of the prediction models and code based DRFs in a quantitative manner, root mean square error (RMSE) and mean absolute error (MAE) are computed for considered period ranges between the target (i.e., determined from code compatible earthquakes) and the prediction models. The results are plotted in Fig. 8. It should be noted that these error measures (i.e., RMSE and MAE) are calculated for NF and FF earthquakes separately and they were averaged for comparison purposes. It can be said that the lower RMSE and MAE can be attributed to less error or biased results, which can be also described as showing better correlation.

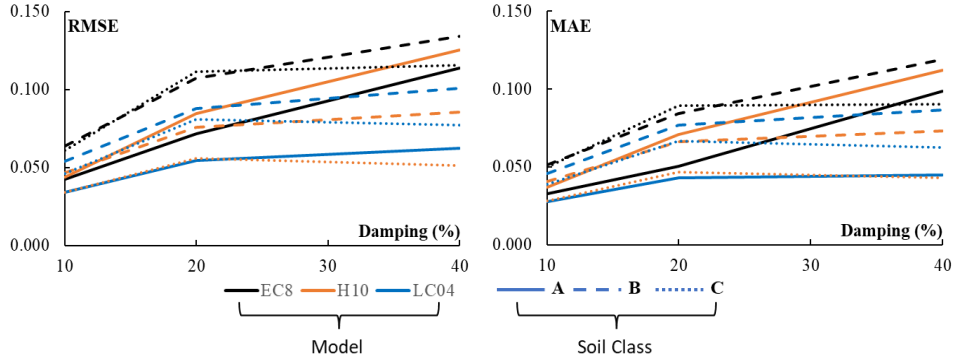

Fig. 8. Comparison of RMSE (left) and MAE (right) distribution of the models in terms of displacement DRFs for different soil classes and damping ratios

It can be viewed from Fig. 8 that values of RMSE and MAE are increasing with increasing damping ratio, in general, and this situation is more apparent with the code-based values. According to the results, LC04 model predictions are less biased compared to H10 and code based DRFs for soil class A. In addition, it seems that H10 model is more biased compared to EC8 for soil class A since the RMSE and MAE values are the average of NF and FF. The evaluations revealed that this situation is mainly related to FF predictions of H10 model as can be also observed in Fig. 5. On the other hand, NF values produced by the H10 model (RMSE < 0.03) is considerably lower than the EC8 model (RMSE >0.04) and the H10 model

(RMSE < 0.06) is less biased compared to EC8 (RMSE > 0.09) and LC04 (RMSE > 0.07) for soil classes of B and C for all damping ratios. In the right side of Fig. 8, MAE results imply that the trends of LC04 and H10 models are almost comparable. It can be said that, in general, H10 and LC04 models are less biased (RMSE < 0.07 and MAE < 0.06 in average) than EC8 DRFs which means a better correlation with DRFs determined from the selected real earthquakes.

In Figure 9, the ratio of DRFd values, for NF and FF earthquakes are plotted for all damping ratios and soil types considered. It can be observed from the figures that despite the fluctuations between the ratios, the ratio shown for soil class B differs significantly from those of soil A and soil B, especially for T > 1.5s. The discrepancies between the ratios increase as the damping ratio increases. The maximum values of the ratios determined from class B are 1.20, 1.45 and 1.71 for 10, 20, and 40% ratios, respectively. The results also align with Lin & Chang [30] model for soil B.

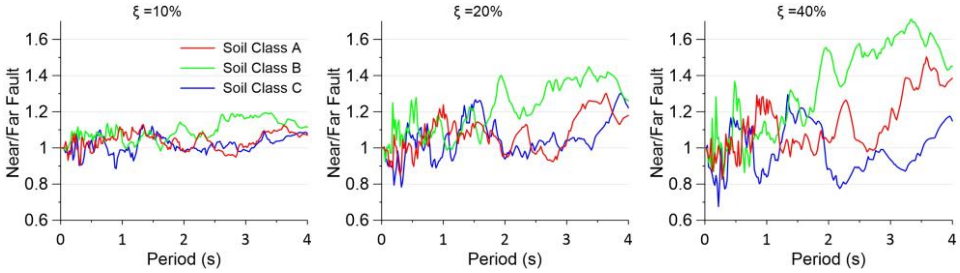

Fig. 9. Comparison of DRFd ratios of near/far-fault earthquakes for ξ = 10%, 20% and 40%

3.3 Effect of Near- And Far-Fault Ground Motions on the DRFa

The effect of NF and DD motions is also examined for acceleration spectra based DRF values considering different damping ratios and A, B and C soil classes defined in EC8. Figures 10 to 12 show the distribution of code based DRFa values according to damping ratios and for NF and FF earthquakes corresponding to A, B and C classes, respectively. The distribution of DRFa values in Figure 10 indicates that the LC04 model is almost compatible with the target DRFs even at high damping ratios regarding site class A.

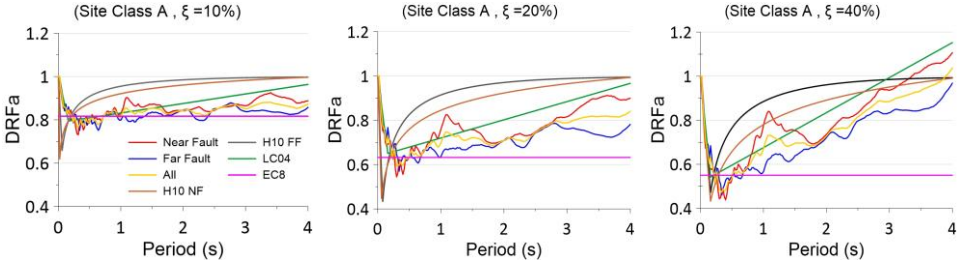

Fig. 10. DRFa values for NF and FF earthquakes for soil A

However, the H10 model produced larger values than the target DRFa values for all damping ratios and for near- and far-fault earthquakes. As observed in earlier section, DRFs produced by EC8 are constant and the code based DRFs seem consistent with DRF values determined from the selected earthquakes. However, compatibility of code based DRF values are significantly decreasing with increasing period, especially high periods (e.g., T > 1.0s).

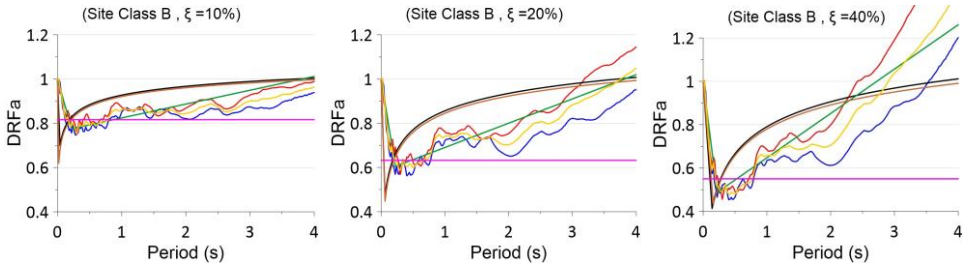

Fig. 11. DRFa values for NF and FF earthquakes for soil B

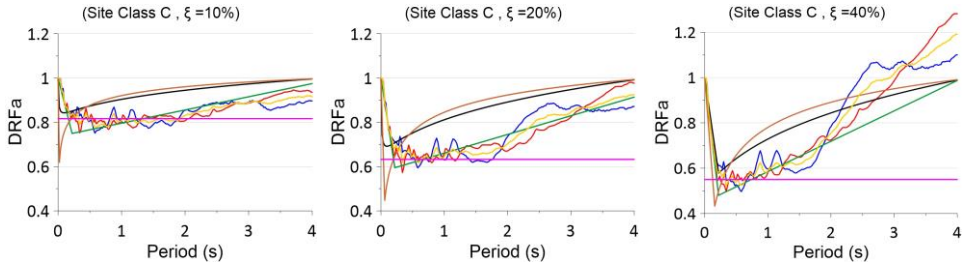

Fig. 12. DRFa values for NF and FF earthquakes for soil C

The distribution of DRFa values corresponding to soil B (see Figure 11) is also similar to the distribution observed for soil A. It can be said that the distribution of DRF values determined from the acceleration spectra is smoother than DRF values determined from the displacement spectra. The effect of NF and DD can also be seen for soil class B, but DRFa values are higher than those of DFRd. The same observations given for soils A and B can also be made for soil class C (see Figure 12). In addition, it can be said that compatibility of H10 model is slightly increasing compared to DRF values for A and B classes, and the values determined from the analysis.

The DRFd values are always lower than the unit value for all soil types and damping ratios. However, DRFa values may be higher than the unit value (i.e., DRFa > 1.0) at high vibration periods (for example for T > 2.5s). When the code based DRFs are evaluated with target DRFa values, it can be said that the code-based results are generally lower than the computed DFRa values and this issue becomes more apparent at high damping ratios. Despite the slight fluctuations computed from the code compatible real earthquakes, especially at low to medium structural periods (T < 2.0s), the code-based values seem to be relatively compatible with DRFa values at low damping ratios (i.e., 10%). On the other hand, the code based DRF values are quite lower than target DRFs for all soil classes and periods higher than 2.0s with increasing damping ratios.

RMSE and MAE are also computed for DRFa values to compare the compatibility of model results with target values and so these are plotted in Fig. 13. It is apparent from both error measures that the LC04 model is consistently less biased (RMSE < 0.1 and MAE < 0.1) compared to H10 and EC8 model DRFs for all soil classes and damping ratios. According to RMSE and MAE results, the H10 model is more biased especially for ξ = 10% compared to EC8 for all soil classes. Similar observations were also made for DRF values determined from displacement spectra, but the biases became more pronounced when DRFa values are used. This situation can be again attributed to the considerations of very short period region (T < 0.50s). Nevertheless, it should be noted that EC8 produces more biased result as the soil becomes softer (RMSE > 0.2 and MAE > 0.2 for soil class of B and C). MAE results (i.e., right side of Fig. 13) also confirm the conclusions drawn from RMSE results. When RMSE and MAE values determined from DRFd and DRFa results are compared (i.e., Fig. 8

and Fig. 13), it can be said that DRFa values are more biased than DRFd values since RMSE and MAE values are higher.

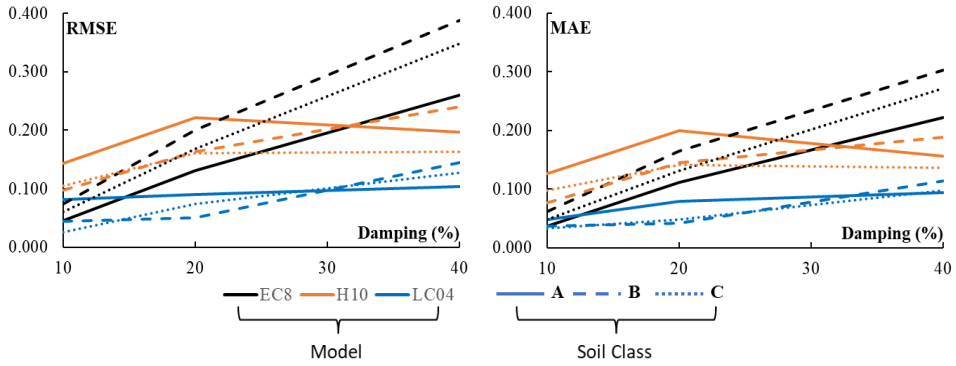

Fig. 13. Comparison of RMSE (left) and MAE (right) distribution of the models in terms of acceleration DRFs for different soil classes and damping ratios

The comparison of DRFa values between NF and FF motions, for various damping ratios and soil classes, is drawn in Figure 14. The curves show that the ratios fluctuated in the short to medium period ranges, such as 0.02 to 1.50s. At high period values (i.e., T > 1.5s), DRFa curves are smoother and the ratios of near/far fault for soil B are higher than for other soil types mainly when the damping ratio increases. In general, the near/ far fault ratios increase with increasing damping ratio and range between 0.9 and 1.1, 0.85 and 1.2, and 0.8 and 1.4 for ξ = 10%, 20% and 40%, respectively.

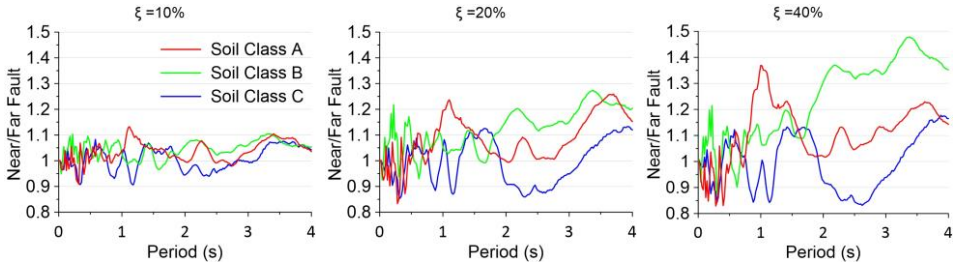

Fig. 14. Comparison of DRFa ratios of near/ far-fault earthquakes for ξ = 10%, 20% and 40%

4. Conclusions

In this study, DRFs were calculated based on the code-based target spectrum. The EC8 design acceleration spectra were used as the target for the ground motion selection. Therefore, real ground motion records were collected from different ground motion databases and divided into two groups, based on epicentral distance to represent the near- and far-fault type earthquakes. Then, the ground motions were selected and scaled to match the EC8 spectra regarding the A, B and C soil types defined in the code. The damping reduction factors were calculated based on the displacement and acceleration response spectra for damping ratios of 10, 20, and 40%, and compared with EC8 and two known DRF models from the literature for evaluation purposes. The following implications can be made:

- The distribution of DRF values indicated that the DRFa results are smoother than those of DRFa over the natural periods. The results also highlighted that DRF

values are more sensitive to ground motion type, vibration period and damping ratios.

- It was observed that the local site conditions have limited effect on DRFs. However, it was found that the DRF ratios of near- to far- field determined from acceleration and displacement spectra are especially exaggerated on site class B. This aligns with the conclusions made by Lin and Chang [30].
- It was observed that DRFd values determined from near-fault type notions are generally higher than those of far- fault type motions around 16, 38 and 58% on average for ξ=10; 20 and 40%, respectively. In addition, it was found that the ratio of DRFd/DRFa is around 1.25 on average, implying the higher DRFd values.
- To evaluate and then compare the code-based and predictions of known models (i.e, H10 and LC04), RMSE and MAE error measures were computed. The computations indicated that regardless of model, soil type and damping ratio, DRFa values (RMSE ≈ 0.145) were more biased then DRFd (RMSE ≈ 0.075) values.
- Based on the measurements, it was noted that LC04 (RMSE ≈ 0.066) and H10 (RMSE ≈ 0.067) models were comparable on average and less biased compared to EC8 (RMSE ≈ 0.091) in terms of DRFd. MAE results also confirm this observation (MAE≈ 0.055, 0.057 and 0.074 for LC04, H10 and EC8, respectively).
- Based on the comparisons, it can be stated that the DRF values provided by EC8 are more biased and the difference between the target and code based DRF values increases as the soil becomes softer, such as RMSE > 0.2 and MAE > 0.2 for soil classes B and C for DRFa. Accordingly, it is thought that code-based definitions should be refined to consider important parameters that affect DRFs.

It should be noted that, although the number of selected records recommended by EC8 is satisfied, the required number of records complying with the code-based record selection recommendations and complying with the near- and far- fault earthquakes were not adequate. Due to the insufficient number of ground motion records, only 15 earthquake records could be selected, for which DRF values were evaluated. However, in future studies, complying code-compatible records other than near- and far- field ground motions could be considered to increase the number of sets including seven or more ground motions to make further evaluations of code-based DRF values.

Acknowledgement

The Institute for Infrastructure & Environment of Heriot-Watt University, Edinburgh, is deeply acknowledged for hosting the main author as Visiting Scholar.

References

[1] Atkinson GM, Pierre J-R. Ground-motion response spectra in eastern North America for different critical damping values. Seismol Res Lett. 2004;75(4):541-545. https://doi.org/10.1785/gssrl.75.4.541

[2] Hatzigeorgiou GD. Damping modification factors for SDOF systems subjected to near-fault, far-fault and artificial earthquakes. Earthq Eng Struct Dyn. 2010;39(11). https://doi.org/10.1002/eqe.991

[3] Hao A, Zhou D, Li Y, Zhang H. Effects of moment magnitude, site conditions and closest distance on damping modification factors. Soil Dyn Earthq Eng. 2011;31(9):1232-1247. https://doi.org/10.1016/j.soildyn.2011.05.002

[4] Newmark NM, Hall WJ. Seismic design criteria for nuclear reactor facilities. In: Proceedings of the 4th World Conference on Earthquake Engineering. 1969. Vol. 4, p. 37-50.

[5] Newmark NM, Hall WJ. Earthquake spectra and design. Eng Monogr Earthq Criteria. 1982.

[6] Comartin CD. Seismic evaluation and retrofit of concrete buildings. Vol. 40. Seismic Safety Commission, State of California; 1996.
[7] Federal Emergency Management Agency. NEHRP guidelines for the seismic rehabilitation of buildings. FEMA-273. Washington DC; 1997.
[8] UBC. Uniform Building Code. International Conference of Building Officials, Whittier, CA; 1994, 1997.
[9] ASCE. Minimum design loads for buildings and other structures. ASCE/SEI 7-05. Reston, Va; 2006.
[10] Federal Emergency Management Agency. NEHRP prestandard and commentary for the seismic rehabilitation of buildings. FEMA-356. Washington DC; 2000.
[11] Kawashima K, Aizawa K. Modification of earthquake response spectra with respect to damping. Doboku Gakkai Ronbunshu. 1984;1984(344):351-355. https://doi.org/10.2208/jscej.1984.351
[12] Caltrans, California Department of Transportation. Seismic Design Criteria, 1.4. Sacr., Cal.; 2006.
[13] Ashour SA. Elastic seismic response of buildings with supplemental damping. University of Michigan; 1987.
[14] UBC-94. Uniform Building Code. International Conference of Building Officials, Whittier, CA; 1994.
[15] Federal Emergency Management Agency. Recommended Provisions for Seismic Regulations for New Buildings. Washington, DC; 1994.
[16] Bommer JJ, Elnashai AS, Weir AG. Compatible acceleration and displacement spectra for seismic design codes. In: Proceedings of the 12th World Conference on Earthquake Engineering. 2000. Vol. 8.
[17] Eurocode 8: Design of structures for earthquake resistance-part 1: general rules, seismic actions and rules for buildings. Brussels Eur Comm Stand. 2005.
[18] Ramirez OM. Development and evaluation of simplified procedures for the analysis and design of buildings with passive energy dissipation systems. State University of New York at Buffalo; 2001.
[19] Federal Emergency Management Agency. Recommended provisions for seismic regulations for new buildings and other structures. NEHRP-2003. Washington, DC; 2003.
[20] S., Otani K. Japanese state of practice in design of seismically isolated buildings. In: The Fourth U.S.-Japan Workshop on Performance-Based Earthquake Engineering Methodology for Reinforced Concrete Building Structures; Sep. 2002.
[21] Ministry of Vehicle Infrastructure and Transport. Guidelines for Calculation Procedure and Technical Standard on Seismically Isolated Structures (in Japanese). Building Center of Japan; 2001.
[22] Priestley MJN. Myths and fallacies in earthquake engineering. Concr Int. 1997;19(2):54-63.
[23] Zhou F, Wenguang L, Xu Z. State of the art on applications, R&D and design rules for seismic isolation in China. In: Proceedings of the 8th World Seminar on Seismic Isolation, Energy Dissipation and Active Vibration Control of Structures. 2003. p. 6-10.
[24] China Code. Seismic Design Code for Buildings (GB 50011-2001). China Archit Ind Press. Beijing, China; 2001.
[25] Benahmed B. Formulation of damping reduction factor for the Algerian seismic code. Asian J Civ Eng. 2018;19(4). https://doi.org/10.1007/s42107-018-0023-6
[26] National Center of Earthquake Applied Research (CGS). Re'gles Parasismiques Alge'riennes., RPA99 (2003 Version). D.T.R. -B.C. 2.48. Algiers, Algeria; 2003.
[27] Hubbard DT, Mavroeidis GP. Damping coefficients for near-fault ground motion response spectra. Soil Dyn Earthq Eng. 2011;31(3):401-417. https://doi.org/10.1016/j.soildyn.2010.09.009

[28] Pu W, Kasai K, Kabando EK, Huang B. Evaluation of the damping modification factor for structures subjected to near-fault ground motions. Bull Earthq Eng. 2016;14(6). https://doi.org/10.1007/s10518-016-9885-8
[29] Li H, Chen F. Damping modification factors for acceleration response spectra. Geod Geodyn. 2017;8(5). https://doi.org/10.1016/j.geog.2017.04.009
[30] Lin Y-Y, Chang K-C. Effects of Site Classes on Damping Reduction Factors. J Struct Eng. 2004;130(11):1667-1675. https://doi.org/10.1061/(ASCE)0733-9445(2004)130:11(1667)
[31] Zhao JX, et al. Effects of earthquake source, path, and site conditions on damping modification factor for the response spectrum of the horizontal component from subduction earthquakes. Bull Seismol Soc Am. 2019;109(6):2594-2613. https://doi.org/10.1785/0120190105
[32] Fernandez-Davila VI, Mendo AR. Damping modification factors for the design of seismic isolation systems in Peru. Earthq Spectra. 2020;36(4). https://doi.org/10.1177/8755293020926189
[33] American Society of Civil Engineers. Minimum design loads and associated criteria for buildings and other structures. 2017.
[34] Benahmed B, Moustafa A, Badaoui M. Comparison between DRF for displacement and acceleration spectra with uncertain damping for EC8. J Mater Eng Struct «JMES». 2019;6(3):345-358.
[35] Abdelhamid A, Benahmed B, Palanci M, Aidaoui L. Assessment of uncertainties in damping reduction factors using ANN for acceleration, velocity and displacement spectra. Electron J Struct Eng. 2023;8-13. https://doi.org/10.56748/ejse.23395
[36] Pavlou EA, Constantinou MC. Response of elastic and inelastic structures with damping systems to near-field and soft-soil ground motions. Eng Struct. 2004;26(9):1217-1230. https://doi.org/10.1016/j.engstruct.2004.04.001
[37] Daneshvar P, Bouaanani N. Damping modification factors for eastern Canada. J Seismol. 2017;21(6). https://doi.org/10.1007/s10950-017-9678-9
[38] Dávalos H, Miranda E, Bantis J, Cruz C. Response spectral damping modification factors for structures built on soft soils. Soil Dyn Earthq Eng. 2022;154. https://doi.org/10.1016/j.soildyn.2022.107153
[39] Zhang H, Zhao YG. Damping Modification Factor of Acceleration Response Spectrum considering Seismological Effects. J Earthq Eng. 2022;26(16). https://doi.org/10.1080/13632469.2021.1991521
[40] Fiore A, Greco R. Influence of Structural Damping Uncertainty on Damping Reduction Factor. J Earthq Eng. 2022;26(4). https://doi.org/10.1080/13632469.2020.1747573
[41] Dicleli M, Kara E. Damping reduction equation for the equivalent linear analysis of seismic isolated structures subjected to near fault ground motions. Eng Struct. 2020;220. https://doi.org/10.1016/j.engstruct.2020.110834
[42] Zhou J, Zhao JX. A damping modification factor prediction model for horizontal displacement spectrum from subduction slab earthquakes in Japan accounting for site conditions. Bull Seismol Soc Am. 2020;110(2):647-665. https://doi.org/10.1785/0120190156
[43] Miranda S, Miranda E, de la Llera JC. The effect of spectral shape on damping modification factors. Earthq Spectra. 2020;36(4). https://doi.org/10.1177/8755293020936691
[44] Ambraseys NN, et al. Dissemination of European strong-motion data, Volume 2. 2004.
[45] Ancheta TD, et al. NGA-West2 database. Earthq Spectra. 2014;30(3):989-1005. https://doi.org/10.1193/070913EQS197M
[46] Kayhan AH, Demir A, Palanci M. Multi-functional solution model for spectrum compatible ground motion record selection using stochastic harmony search algorithm. Bull Earthq Eng. 2022;20(12):6407-6440. https://doi.org/10.1007/s10518-022-01450-8

[47] Demir A, Palanci M, Kayhan AH. Evaluation of supplementary constraints on dispersion of EDPs using real ground motion record sets. Arab J Sci Eng. 2020;45(10):8379-8401. https://doi.org/10.1007/s13369-020-04719-9
[48] Palanci M, Demir A, Kayhan AH. A statistical assessment on global drift ratio demands of mid-rise RC buildings using code-compatible real ground motion records. Bull Earthq Eng. 2018;16(11):5453-5488. https://doi.org/10.1007/s10518-018-0384-y
[49] Kayhan AH, Demir A, Palanci M. Statistical evaluation of maximum displacement demands of SDOF systems by code-compatible nonlinear time history analysis. Soil Dyn Earthq Eng. 2018;115:513-530. https://doi.org/10.1016/j.soildyn.2018.09.008
[50] Demir A, Palanci M, Kayhan AH. Probabilistic assessment for spectrally matched real ground motion records on distinct soil profiles by simulation of SDOF systems. Earthquakes Struct. 2021.
[51] Palanci M, Demir A, Kayhan AH. The investigation of displacement demands of single degree of freedom models using real earthquake records compatible with TBEC-2018. Pamukkale Üniversitesi Mühendislik Bilim Derg. 2021;27(3):251-263. https://doi.org/10.5505/pajes.2020.47936
[52] Graizer V, Kalkan E. Prediction of spectral acceleration response ordinates based on PGA attenuation. Earthq Spectra. 2009;25(1):39-69. https://doi.org/10.1193/1.3043904
[53] Demir A, Palanci M, Kayhan AH. Evaluation the effect of amplitude scaling of real ground motions on seismic demands accounting different structural characteristics and soil classes. Bull Earthq Eng. 2023. https://doi.org/10.1007/s10518-023-01780-1
[54] Palanci M, Demir A, Kayhan AH. Quantifying the effect of amplitude scaling of real ground motions based on structural responses of vertically irregular and regular RC frames. In: Structures. 2023. Vol. 51, p. 105-123. https://doi.org/10.1016/j.istruc.2023.03.040
[55] Demir A, Kayhan AH, Palanci M. Response-and probability-based evaluation of spectrally matched ground motion selection strategies for bi-directional dynamic analysis of low-to mid-rise RC buildings. In: Structures. 2023. Vol. 58, p. 105533. https://doi.org/10.1016/j.istruc.2023.105533
[56] Bommer JJ, Acevedo AB. The use of real earthquake accelerograms as input to dynamic analysis. J Earthq Eng. 2004;8(spec01):43-91. https://doi.org/10.1080/13632460409350521
[57] Chopra AK. Dynamics of structures. Pearson Education India; 2007.